

1
2
3
4
5
6
7
8

Accepted version
Licence CC BY-NC-ND
Please cite as:

Surricchio G., Pompilio L., Arizzi Novelli A., Scamosci E., Marinangeli L., Tonucci L., d'Alessandro N., Tangari A.C. (2019), "Evaluation of heavy metals background in the Adriatic Sea sediments of Abruzzo region, Italy", *Science of the Total Environment*, Vol. 684, pp. 445-457, doi: <https://doi.org/10.1016/j.scitotenv.2019.05.350>

9 **Evaluation of heavy metals background in the Adriatic Sea sediments of Abruzzo**
10 **region, Italy**

11 Giulio Surricchio ^a, Loredana Pompilio ^b, Alessandra Arizzi Novelli ^a, Emanuela Scamosci ^a, Lucia
12 Marinangeli ^b, Lucia Tonucci ^{c,*}, Nicola d’Alessandro ^d, Anna Chiara Tangari ^b

13 ^a Environmental Protection Agency of Abruzzo, Arta Abruzzo, Viale Marconi 178, I-65127 Pescara,
14 Italy

15 ^b Department of Psychological, Health & Territorial Sciences, “G. d’Annunzio” University of Chieti-
16 Pescara, Via dei Vestini, I-66100 Chieti, Italy

17 ^c Department of Philosophical, Educational and Economic Sciences, “G. d’Annunzio” University of
18 Chieti-Pescara, Via dei Vestini, I-66100 Chieti, Italy

19 ^d Department of Engineering and Geology, “G. d’Annunzio” University of Chieti-Pescara, Via dei
20 Vestini, I-66100 Chieti, Italy

21
22
23 Corresponding author: lucia.tonucci@unich.it (L. Tonucci)

24
25 **Abstract**

26 This work focuses on the characterization of background levels of heavy metals (As, Cd, Cr, Cu, Hg,
27 Ni, Pb, Zn) in seabed marine sediments of the central Adriatic Sea, collected up to 10 km far from the
28 Abruzzo region coastline (Italy). The used approach follows the guidelines established by the Decree of
29 the Italian Ministry of Environment, n. 173/2016, concerning the determination of threshold values of

30 metal concentration, and including only samples with low or absent toxicological content. A statistical
31 analysis, using the adjusted Tuckey's boxplot to identify the percentiles and potential outliers, was
32 performed. The background concentrations were calculated as the values of the 90th percentile of
33 distribution, according to the national regulation. This study represents the first attempt to calculate the
34 background levels of marine sediments done at regional level in Abruzzo. A few outliers have been
35 found, and interpreted as potential anthropic contamination.

36

37 **Keywords:** hazard metals, Adriatic Coast, seabed sediments, background level.

38

39

40 **Highlights**

- 41 • Background of heavy metals in central Adriatic Sea, according to environmental laws
- 42 • As, Cd, Cr, Cu, Hg, Ni, Pb, and Zn have been quantified in 110 sediment samples
- 43 • Anomalous values have been identified through univariate and multivariate statistics
- 44 • 90th percentile has been used to identify the metal local background L_{10c}

1. Introduction

45 The maintenance and management of coastal environments generally deal with the handling and reuse
46 of marine sediments, especially after dredging operations have been accomplished. Many human
47 activities involve mobilization of materials from the seabed, such as dredging for ensuring safe
48 navigation, maintenance of port facilities, coastal defence from erosion, flood mitigation, etc.

49 (Carpenter et al., 2018). Once excavated, marine sediments can be commonly used for beach
50 nourishment purposes or disposed offshore. The importance of this matter is straightforward in the
51 context of socio-economic organization of coastal populations (Dinwoodie et al., 2012). Nevertheless,
52 it has a remarkable prominence as regards the environmental protection actions to be implemented in
53 order to reduce environmental threats and hazards.

54 The remarkable importance of the argument is demonstrated by the existence of explicit regulations
55 addressing the specific point of marine sediments handling and reuse. The final destination of sea floor
56 sediments is certainly dependent on their contamination levels, according to national regulations. In
57 Italy, the most recent regulation concerning terms and technical criteria for the authorization to dump
58 the dredged sediments in the marine environment, is the Decree of the Italian Ministry of Environment,
59 n. 173/2016, which is in force from the 21st September 2016. The decree n.173/2016 establishes criteria
60 and methods for the characterization and classification of seabed sediments, and the technical
61 requirements for the management and disposal at sea. It also provides the national reference chemical
62 thresholds for both organic and inorganic contaminants in sediments. Threshold L_1 is the concentration
63 of an element or compound at which toxicity and bioaccumulation effects occur with poor probability
64 (decree n.173/2016). The regulation allows to use local L_1 (L_{1loc}) thresholds when available.

65 The “Manual on marine sediments handling” (APAT-ICRAM, 2007) also includes a review of
66 sampling techniques and analytical methods to be applied to marine sediments prior to their reuse. Both
67 references are valid within the Italian marine environments and both deal with the theme of the quality
68 assessment of sediments based on the concept of weight of evidence, which integrates data from
69 different studies to address the presence of chemical pollutants, their bioavailability, and the onset of
70 adverse effects in selected organisms (Piva et al., 2011). Ecotoxicology is an important detection tool
71 supporting the traditional chemical analysis to evaluate the pollution risk associated to complex solid

72 matrices (*e.g.*, harbour and dredging sediments). It reveals, in fact, the bioavailability of potential
73 pollutants in the real samples but, as such, it is not able to identify the agent responsible of the positive
74 effect. The use of biological indicators is becoming very important in evaluating the quality of
75 sediments and their potential effects on the environment (Volpi Ghirardini et al., 2005; Picone et al.,
76 2016).

77 Chemical characterization by itself does not provide specific biological information about potential
78 hazards to organisms. In addition, both the magnitude and extent of contamination may only be
79 assessed when the natural levels of contaminants are known (Birch, 2017). It is recognised that the
80 chemical composition of source rocks strongly affect the geochemistry of sediments (Bábek et al.,
81 2015). Also, sediment texture, mineralogical composition, organic carbon content, reduction/oxidation
82 state, adsorption and desorption processes have influence on both the mobility and availability of
83 metals in marine sediments (Lopes-Rocha et al., 2017a; Cortecchi et al., 2008). Matys Grygar and
84 Popelka (2016) reviewed the effects of several exogenic processes that can produce element patterns
85 different from those of the catchment rocks, thus causing a natural enrichment of some elements such
86 as organic matter content, grain size or neo-formation of fine particles during transport through the
87 catchment which may undergone further chemical transformations due to reductive/oxidative-driven
88 processes. As a result, the knowledge of the so-called “geochemical background”, according to the
89 definition of Matschullat et al. (2000), has a fundamental relevance in environmental studies and
90 sediment management operations.

91 Numerous techniques to define the geochemical background have been employed in contamination
92 studies of marine sediments (Covelli and Fontolan, 1997; De Lazzari et al., 2004; Reimann and Garrett,
93 2005; Abraham and Parker, 2008; Heimbürger et al., 2012; Felja et al., 2016; Birch, 2017, and

94 references therein). A general distinction between geochemical and statistical methods can be made
95 (Matschullat et al., 2000; Bábek et al., 2015; Birch, 2017), but the approaches to determine the regional
96 background are always based on: a) sampling pristine sediments; b) sampling datable long sediment
97 cores; c) sampling a large number of sites (Rodríguez et al., 2006). So far, detailed investigations of
98 contamination degree and sediment provenance have been accomplished in particular in the Northern
99 and Southern sectors of the Adriatic Sea (Covelli and Fontolan, 1997; Dinelli and Lucchini, 1999; De
100 Lazzari et al., 2004; Harris et al., 2008; Goudeau et al., 2013; Romano et al., 2013; Ilijanić et al., 2014;
101 Migani et al., 2015; Langone et al., 2016; Natali and Bianchini, 2018). The middle Adriatic sector has
102 been investigated by Spagnoli et al. (2014), and Lopes-Rocha et al. (2017a and b) and references
103 enclosed therein. However, only few samples from the Central Adriatic seabed, including samples
104 collected in cores, are available from previous studies and they are not sufficient to establish a local
105 background.

106 The main goal of this work is to determine the local background (L_{loc}) of trace metals such as As, Cd,
107 Cr, Cu, Hg, Ni, Pb, and Zn in marine sediments collected along-shore of the Abruzzo region (Fig. 1), at
108 a distance between 0.5 and 10 km from the coastline, following the indications provided in the national
109 regulation n. 173/2016, and then critically analysing the results. The assessment of these reference
110 values will allow either the regulatory and monitoring bodies to better manage all the human activities
111 related to excavation and handling of marine sediments, and to avoid diffusion of local contamination.

112

2. Materials and Methods

2.1. Study area

113
114 The Adriatic Sea is a narrow and mostly shallow epicontinental basin extending NW-SE for more than
115 800 km and with an average width of about 200 km. The northern Adriatic consists of a broad shelf
116 with depths shallower than 100 m dipping toward the Middle Adriatic Depression (~270 m deep),
117 which culminate into the Southern Adriatic basin (Langone et al., 2016). The central Adriatic is
118 characterized by a narrow shelf, with a maximum gradient on the order of $0.3 - 0.7^\circ$ (Amorosi et al.,
119 2016), and localised bathymetric irregularities due to structural highs offshore Punta Penna, the Tremiti
120 Islands and the Gargano promontory (Cattaneo et al., 2003).

121 The primary fluvial system entering the Adriatic Sea is the Po river in the northern basin. It has one of
122 the largest drainage basins in Europe and supplies one third of the freshwater input and one fourth of
123 the sediment entering the Adriatic Sea. Additional freshwater inputs come from the Alpine rivers
124 outflowing in the northern sector and a set of small Apennines rivers in the central and southern sectors
125 (Lopes-Rocha et al., 2017a). Sediment input is restricted to the northern and western side of the basin,
126 whereas the eastern supply becomes important only in the southern Adriatic sector (Dinelli and
127 Lucchini, 1999), due to the presence of shore-parallel structural traps and very short and small rivers
128 draining dominantly carbonatic rocks of the Dinaric mountain belt, affected by extensive karstic
129 phenomena (Cattaneo et al., 2003). As a whole, the solid load from the Italian rivers includes terrains
130 of the Eastern Alps (predominantly carbonatic and minor marly flysch and metamorphic lithologies)
131 and of the largest part of the Apennines chain (marls, limestones and sandstones in the northern sector;
132 mainly limestones and dolostones of the Apenninic Mesozoic platform and of the Argille Scagliose
133 formation, together with flysch and sands, clays and marls of the Plio-Pleistocene deposits, in the

134 central and southern sectors), whereas the material derived from the Western and Central Alps is
135 supplied by the Po river (metamorphic rocks of the crystalline basement in the western side; limestones
136 and dolostones from the tributaries of the central course draining the Alps, and shales, marls,
137 sandstones and minor occurrence of mafic and ultramafic rocks of the Ligurian domain, from the
138 tributaries draining the Apennines).

139 The Adriatic basin is characterized by a microtidal regime and dominated by a thermohaline cyclonic
140 circulation which is seasonally modulated by wind forcing with the catabatic Bora wind blowing from
141 the NE during winter and the Scirocco wind blowing from SE during summer. In summer, in the
142 northern and central sectors, the hydrodynamic consists of weak currents resulting in a series of
143 clockwise and counter-clockwise gyres. In winter, counter-clockwise currents parallel to the coastline
144 become dominant and tend to flow near the bottom along the Italian side of the Adriatic Sea (Cattaneo
145 et al., 2003; Amorosi et al., 2016). In addition, the formation of dense waters in the Northern Adriatic
146 Sea that annually or biennially flow southward in spring further complicate the circulation. The main
147 consequence of the general Adriatic circulation pattern is that Mediterranean Sea waters inflow into the
148 Adriatic Sea from the eastern side of the Otranto Strait and the Adriatic waters outflow across the
149 western side of the Otranto Strait (Spagnoli et al., 2014). Water and sediment discharge to the Adriatic
150 basin reaches the maximum during late autumn and late spring (Weltje and Brommer, 2011).

151 The discharge of southern rivers (North of the Gargano promontory) represents a very important
152 sediment source for the entire basin which is double that of the Po river itself, though the size of this
153 drainage areas is less than a half (Cattaneo et al., 2003). The dominant cyclonic circulation traps fresh
154 waters and sediments discharged by the Po and Apennine rivers to a narrow band along the western
155 side of the basin, known as the Western Adriatic Current, which goes down to the Gulf of Taranto
156 (Goudeau et al., 2013). South of the Po river, those currents are responsible for the efficient sediment

157 redistribution in a shore-parallel direction along the Italian coast (Frignani et al., 2005; Amorosi et al.,
158 2016, and references therein). Frignani et al. (2005) demonstrated that in the Northern Adriatic sector
159 (North of Ancona), the sedimentary supply exceeds the accumulation on the seabed, whereas the
160 opposite is true for the central Adriatic. This, in turn, reveals that along-shore sediment transport is
161 very effective and, in particular, about 35% of the riverine supply as a whole is transferred from
162 northern to central Adriatic, through the Ancona transect.

163 The sediment contribution along the Abruzzo coastline is mostly due to several short rivers (mainly
164 Pescara, Sangro and Trigno) and is mostly terrigenous with variable content of carbonaceous nature
165 (Dinelli and Lucchini, 1999; Frignani et al., 2005). These rivers drain a catchment area of about 3000,
166 1500 and 1200 km², respectively, and contribute near 15% of the whole fluvial input of sediments in
167 the Adriatic Sea (Frignani et al., 2005).

168 ***2.2. Sampling and analyses methods***

169 The sampling strategies and performed analyses have been carried out according to standardized
170 procedures (APAT-ICRAM, 2007) and the national regulation n. 173-2016.

171 ***2.2.1. Sampling strategy***

172 Sediment samples were collected from 2011 to 2016 by the Regional Agency for the Environmental
173 Protection (ARTA – Abruzzo) along-shore Abruzzo region, from Martinsicuro to the North up to San
174 Salvo to the South (Fig. 1), during different cruises on board the Ermione ship. Sampling sites
175 distribution is shown in Fig. 1. Seabed sediments have been collected at more than 50 total target sites,
176 and repeated sampling has been carried out once a year at least. Temporal variability is part of the
177 natural variability and thus it should be accounted for in the background determination studies.
178 Temporal variability is generally considered in environmental monitoring programmes, in order to

179 account for sedimentation and/or mobilization processes changes through time. The ARTA–Abruzzo
180 agency has the task to accomplish periodic along-shore sampling campaigns, within the framework of
181 projects addressed to monitoring the level of pollution, characterizing the conditions of water and
182 sediments as well as investigation purposes.

183 The top 15 cm of undisturbed seabed sediments was collected through a “Van Veen” grab sampler
184 within a sampling area of 0.1 m². Sampling has been performed under optimal weather and sea
185 conditions. During sampling operations, at each target site, weather conditions and GPS position have
186 been recorded, as well as sea-water transparency by Secchi disc. Also physical-chemical measurements
187 were carried out on the water column (*i.e.*, temperature, salinity, dissolved oxygen, pH and a-
188 chlorophyll) using the Ocean Seven 316 plus probe (Idronaut). The probe acquired the measurements
189 every 1 m from 0.5 m below the water surface, up to 0.5 m above the sea floor. The real time
190 transmission of the collected data to the onboard operator allows to check the trend of each parameter
191 under the water interface, and thus evaluate eventual anomalies in signal transmission or in the sea
192 conditions, as turbulence or bottom material re-suspension.

193 Once on board, samples were recovered from the bucket with a steel spatula to avoid contamination,
194 homogenized and then stored in specially labelled cans for sediment characterization, chemical and
195 ecotoxicological analyses. For each sample, a set of metadata (station name, date, time, theoretical and
196 real coordinates, instrumentation used) was recorded. Sediment samples for ecotoxicological analyses
197 were placed in decontaminated glass containers, stored in portable refrigerators and transported in the
198 laboratory, at 5±3 °C temperature. Each sample was further homogenized and processed to obtain
199 elutriates for toxicity bioassays within one week from sampling and the whole sediment analyses were
200 carried out within 15 days from sampling.

201 2.2.2. *Chemical analyses*

202 According to the national regulation n. 173/2016, the trace metals concentrations have been measured
203 on the dry material. Dry residue was determined via gravimetric analysis, according to the ISO
204 11465:1993 method. Its principle is drying the samples to constant mass at 105 °C and using the
205 difference in mass of an amount of sediment before and after the drying procedure. Trace elements (As,
206 Cd, Cr, Cu, Ni, Pb, Zn) concentration was defined through Inductively Coupled Plasma–Optical
207 Emission Spectrometry (ICP-OES), using a Varian 720-ES Spectrometer, according to the UNI EN
208 ISO 11885:2009 method. The US EPA 7471B 2007 method, based on Cold Vapor-Atomic Absorption
209 Spectrophotometry (CVAAS), was used for Hg determination.

210 The TOC of the samples were measured by an elemental analyzer (Analytik Jena multi N/C Series)
211 following the UNI EN 15936:2012 method.

212 2.2.3. *Ecotoxicological analyses*

213 The battery of bioassays followed standardized procedures of exposure conditions, matrix and
214 biological endpoint. Selected species were the bacterium *Vibrio fischeri* (acute effects of the sediment
215 as a whole on bioluminescence), the algae *Pheodactylum tricornutum* (chronic effects of elutriate on
216 growth), and the mussel *Mytilus galloprovincialis* (chronic effects of elutriate on larvae).

217 The Microtox Solid Phase Test (SPT) was carried out according to the method described in Appendix 2
218 of the ICRAM (2001) and UNI EN ISO 11348-3 (2009) method, using a Microtox analyser M500
219 (Azur Environmental). The sediment as a whole, and not the centrifuged sediment, has been used,
220 because it represents the more ecologically relevant matrix, according to Onorati and Volpi Ghirardini
221 (2001). EC50 and its 95% confidence range were then calculated.

222 All the tests were carried out on eight dilutions, including negative (artificial seawater) and positive
223 (3,5-dichlorophenol) controls in each experiment. Microtox SPT assay is based on the lowering of the
224 natural *V. fischeri* bioluminescence deriving from the acute toxicity. Application of SPT to marine
225 sediments is important due to its remarkable advantages of measuring the toxicity of the whole
226 sediment and allowing to associate toxicity with the pelitic fraction. The results are expressed as
227 Sediment Toxicity Index (STI), that is the ratio between the measured toxicity and the natural estimated
228 value in relation to the pelitic fraction contained in each sample. Since the sediment toxicity is
229 predominantly associated with the pelitic fraction, as it provides a large adhesion or adsorption surface
230 to the contaminants, STI allows correlation between the possible toxicity which can be found in the
231 granulometric component of <63 μm fraction. Pelitic normalization model proposed with this index is a
232 simple and objective criterion applicable to the evaluation of the acute toxicity of contaminated
233 sediment samples.

234 The remaining tests were carried out using the elutriates, extracted according to the US EPA (1991)
235 standard procedure.

236 As regard the tests on the effects of elutriates, researchers are oriented toward the use of indigenous
237 species as the most representative species for the marine specific areas of concern. In fact *P.*
238 *tricornutum* is a diatom that can be found in coastal and inland waters and it has been shown to be a
239 sensitive organism to heavy metals and other persistent pollutants (*e.g.*, polycyclic aromatic
240 hydrocarbons) exposure.

241 Short-term toxicity test with the *P. tricornutum* was carried out according to ISO 10253 (2016) and
242 Libralato et al. (2011). The exposure of *P. tricornutum* to the metals rich elutriates produces a
243 progressive inhibition of growth, thus providing an indirect proof of the presence of hazardous

244 compounds which are available in the water column as a consequence of sediment resuspension.
245 Experiments were carried out in triplicate, also including negative (artificial seawater) and positive
246 ($K_2Cr_2O_7$) controls. Cell density was assessed using a Bürker counting chamber. A regression line was
247 estimated between the logarithm of blank-corrected cell density and metal concentration. Point
248 estimation and the 95% confidence interval at the concentrations which inhibit the growth were carried
249 out.

250 Mussels, and particularly the autochthonous *M. galloprovincialis*, are considered as the best candidate
251 marine organisms for identification of the potential effects of pollutants in the water column. They are,
252 in fact, considered as good biological indicators both for their sensitivity (using embryotoxicity data)
253 and the ability of discriminating sediments with different levels and types of contamination.
254 Embryotoxicity tests with the bivalves *M. galloprovincialis* were carried out according to ASTM E724
255 - 98 (2012). After eggs fertilization and incubation, the larvae were counted and distinguished between
256 normal (D-shaped) and abnormal (malformed larvae and pre-larval stages) ones. The acceptability of
257 test results was based on negative control for a percentage of D-shaped larvae $\geq 70\%$. Negative
258 (artificial seawater) and positive ($Cu(NO_3)_2$) controls were also included. Three replicates for each
259 sample (nominal concentration for both Cu ion and elutriates) were tested. EC50 values with 95%
260 confidence interval were calculated by Trimmed Spearman-Kärber (Hamilton et al., 1978).

261 2.2.4. Textural and mineralogical analyses

262 According to the national regulation n. 173/2016, the grain size fractions of the gravel (> 2 mm), sand
263 (2 mm $< x < 63$ μ m) and mud (< 63 μ m) have been measured by dry sieving. Mineralogical analyses of
264 the powdered sediments have been performed using the Rigaku Miniflex II X-ray diffractometer
265 (XRD), in order to characterize the primary mineral assemblage. This XRD instrument uses Cu-K α

266 emission at 50 kV and 1 mA and the interpretation of the diffraction patterns has been carried out
267 following Moore and Reynolds (1997).

268 2.2.5. *Statistical analyses*

269 To calculate the local background of trace metals concentration in marine sediments collected along-
270 shore Abruzzo region, the approach recommended by the national regulation n. 173/2016 was
271 essentially followed. According to the decree n. 173/2016, the local background is the 90th percentile of
272 the sample distribution not affected by toxicity effects. Therefore, a subset of the original dataset has
273 been used, including those samples with low or absent STI (see paragraph 2.2.3.).

274 The statistical analysis of trace metals concentrations in marine sediments implies to cope with the
275 different issues of a number of values lower than the instrumental detection limit, and the assessment of
276 putative *vs.* real outliers. Both these data types complicate the familiar computations of descriptive
277 statistics, and in turn the statistical determination of background values. Therefore, they have to be
278 treated properly, although the regulation n. 173/2016 does not provide any indication about these
279 occurrences.

280 Statisticians use the term “censored data” for observations that are not quantified but known to exceed
281 or fall behind a threshold value (Helsel, 2012). Depending on the position of the value with respect to
282 the threshold, data can be considered as left- or right-censored. The dataset used in this study, include
283 only left-censored observations, reported as semi-numerical values indicating that the analyte is below
284 the laboratory’s detection limits. Those measurements are considered too imprecise to report as a single
285 number, so the value is commonly reported as being less than an analytical threshold.

286 Several data-analysis procedures are available for censored data. According to Lee and Helsel (2005),
287 these procedures are referred to as simple-substitution methods, parametric methods, and

288 nonparametric methods. According to Helsel (2012), ignoring or substituting the values tied to the
289 reporting limits with arbitrary quantitative values is not a reasonable method for interpreting censored
290 data. Parametric methods require sufficient data to validate the use of a specific distributional model.
291 Nonparametric methods do not require the assumption of a specific distribution to estimate summary
292 statistics for multiply censored datasets. In between parametric and nonparametric, there is a “robust”
293 semi-parametric method developed by Helsel and Cohn (1988). This method is an implementation of
294 what is generally referred to as a regression on order statistics or ROS (Lee and Helsel, 2005). Among
295 the several software tools that perform robust linear ROS, a library called NADA (Helsel, 2005), which
296 is developed as an add-on package for the R environment for statistical computing (R Core Team,
297 2018), has been used to generate summary statistics, plot modelled distributions, and predict or
298 estimate modelled values based on the modelled distributions.

299 The definition of outliers from a distribution is not unique nor absolute but it is strongly dependent on
300 data distribution and is also influenced by the purpose of the analysis. As long as outliers do not
301 influence assumptions of a statistical test, and are recognized as incidental or potential occurrence, one
302 can identify them and explain their significance. In the present study, two different methods were used
303 in order to detect outliers in the dataset: the Tukey’s method (Tukey, 1977), and the adjusted boxplot of
304 Hubert and Vandervieren (2008).

305 Tukey’s boxplot is a well-known graphical tool to display information about continuous univariate
306 distributions. Boxplots are one of the most intuitive ways to visualize a data set. They employ three
307 percentiles (25th, 50th, and 75th) that define the central box. The relative positions of the percentiles
308 show the centre, spread, and skewness of the data. Tukey’s method is less sensitive to extreme values
309 than the methods using the sample mean and standard variance and is applicable to skewed
310 distributions since it makes no distributional assumptions and it does not depend on a mean or standard

311 deviation. According to the Tukey's method, the distance between the lower (Q_1) and upper (Q_3)
312 quartiles is the IQR (Interquartile Range), the inner fences are located at [$Q_1 - 1.5 \text{ IQR}$, $Q_3 + 1.5 \text{ IQR}$],
313 and the outer fences are located at [$Q_1 - 3 \text{ IQR}$, $Q_3 + 3 \text{ IQR}$]. A value between the inner and outer
314 fences is a possible outlier, while an extreme value beyond the outer fences is a probable outlier.

315 The adjusted boxplot method includes a robust measure of skewness in the determination of the
316 whiskers, thus allowing a more accurate representation of the data and of possible outliers, according to
317 Hubert and Vandervieren (2008). Both the methods can be used as fast and automatic outlier detection
318 tools without making any parametric assumption about the distribution of data.

319 In order to account for possible different processes and/or physic-chemical conditions affecting the
320 distribution of elements in the dataset, multivariate statistics has been also carried out (Mali et al.,
321 2015, and references therein). Principal Component Analysis (PCA) on scaled and centred data was
322 performed with the aim of understanding the structure of data and, eventually, their variations and
323 patterns. Due to the variable number of missing (NA) and left-censored values in the dataset, the set of
324 variables with the largest availability (metals and mud fraction) has been used. According to
325 Stanimirova (2013), replacement with half of the reporting limits, although inappropriate in univariate
326 statistics, is widely used for dealing with left-censored data in multivariate analyses, and this practice
327 has a negligible effect on PCA performance when the value of censored elements per variable does not
328 exceed 20%. Therefore, the variables Hg and TOC has been excluded from the analysis, while As and
329 Cd have been considered by replacing the left-censored measurements with half of the reporting limits.
330 Mineralogical data have not been included in PCA analysis, according to the scattered availability of
331 the measurements.

332 All the computations described above have been developed using the freely available R environment
333 for statistical computing (<http://www.r-project.org>).

334

3. Results and Discussion

335 According to the results of the ecotoxicological analyses described in paragraph 2.2.3., a subset of 110
336 out of 297 total samples, collected during the time span between 2011 and 2016, has been used in
337 statistical analyses. These 110 samples were considered suitable for the trace elements background
338 computation, since they did not show ecotoxicological danger for the observed living organisms. The
339 list of samples, localization and analyses results is reported in Table 1 including the grain size when
340 available.

341 Major elements (*e.g.*, Mg, K, Si, Ti, Zr) have not been measured, while Al, Zn, and V have many
342 missing values. Also, pH and redox potential have not been provided by the collector. The scattered
343 availability of some measurements depends on the fact that the surveys carried out by ARTA-Abruzzo
344 address different objectives and thus the agency is not required to provide always the same set of
345 analyses. Table 1 also shows a number of measurements of As, Cd, and Hg content falling below the
346 instrumental detection limits and therefore not accountable using the traditional parametric univariate
347 statistics. Those measurements have been treated as described in paragraph 2.2.5.

348 Mineralogical analyses were provided for a limited subset of samples collected during the 2016
349 campaigns (Table 2) and compared with the data collected during the PRISMA campaign in 1995
350 (Spagnoli et al., 2014) in this area. Spagnoli et al. (2014) classified the Abruzzo coastal sediments as
351 part of the “Padanic Facies” where the sedimentary load of the Po river is mixed with the Apennine
352 rivers one. A significant variation of the quartz, dolomite and plagioclase content is observed. It should

353 be noted that, compared to the PRISMA dataset, the samples used in this study are closer to the
354 shoreline, where the influence of the local fluvial sediment discharge is stronger. This is confirmed by
355 the coarser grain size (~70% sand in average) compared to the PRISMA samples which are mostly
356 clay-rich. Based on the coarse grain size and strong enrichment of quartz, the seabed sediments used in
357 this study likely result from a mixture of fluvial discharge and submerged beaches deposits.

358 As expected, the content of trace metals is proportional to the amount of fine sediment as shown in
359 Figure 2.

360 A subset of samples has been used to compare the variation of main mineralogical species (Quartz,
361 Calcite and Dolomite), granulometry and total organic content (Fig. 3). The overall distribution is
362 consistent with the marine coastal dynamics of sedimentation with decreasing granulometry offshore. It
363 is interesting to observe that the Casalbordino's samples are generally more homogenous and richer in
364 clay and carbonates, except for the sand-rich sample PE/005831/2016 which may be related to the
365 presence of coastal sandy barrier. It should also be noted that sample PE/005831/2016 correlates quite
366 well with sample PE/005973/2016 to the North and both sites are at the same distance from the
367 coastline. Strong anomalies are represented by samples PE/005974/2016 and PE/005975/2016, both
368 having the highest mud content. This may be explained by their large distance from the shoreline;
369 however it is worthwhile to note that these sites represent also the Pb and Cd outliers in the 2016
370 campaign. Given the lack of granulometry information for each campaign, it is not straightforward to
371 establish whether the high mud content of these samples is due to a normal sedimentation, and it is
372 something to further investigate in the future.

373 To account for both the statistical and spatial distribution of the measurements within the dataset,
374 Tukey's boxplots, density diagrams (only uncensored data) and the maps of distribution per element

375 (Fig. 4) have been employed. The target measurements are represented with circles whose size varies
376 depending on quartiles and the distance from the whiskers, to quickly highlight distribution patterns
377 and outliers. For this statistical approach the different date of campaigns for sample collection is not
378 significant, but it may become important to understand the presence of outliers.

379 The concentrations of chemical species in seabed sediments show strongly skewed distributions. The
380 density diagrams of Ni, Zn, Pb, Cr, and Cu (Fig. 4) also show multimodal distributions of the data
381 records. Environmental data often exhibit non-normal behaviour and the measurements are frequently
382 positively skewed and multimodal, as already observed in previous studies (Matschullat, 2000; Helsel,
383 2012; Birch, 2017). According to the observed behaviour, the use the of the Tukey's boxplot graphical
384 representation allows to quickly identify extreme values.

385 The approach described by Hubert and Vandervieren (2008), which includes the computation of a
386 robust measure of skewness in the determination of the whiskers has also been used. However, the
387 improvement achieved using adjusted boxplots over Tukey's ones is not persuasive because a) the
388 adjusted boxplot often increases the risk of swamping, that is the misclassification of an observation as
389 an outlier and b) the results are often identical when the outer fences are used as discriminating limits.
390 The adjusted boxplot of Hubert and Vandervieren (2008) is much more vulnerable to swamping
391 especially toward lower values. Since the main goal of this investigation is to find the realistic
392 background level of trace elements concentration, the hypothesis of finding outliers in the lower
393 portion of data distribution is rejected. As regard to point b), a major difference is observable only in
394 the case of Cu (Fig. 4e) where the Tukey's boxplot allows to identify a single outlier while the adjusted
395 boxplot includes that value within the main distribution.

396 The case of Cu is peculiar because, as shown in Fig. 4e, the density diagram shows a multimodal
397 distribution, with a clear single extreme value which strongly appears as an anomaly. The specific
398 measurement refers to sample PE/003340/2012 (see Table 1) which has been collected about 500 m
399 offshore from the Alento river mouth, during August 2012 campaign. The other sampling points
400 located at similar distance from the shore and in the nearby of point PE/003340/2012 have been
401 collected three years later, and they show Cu concentrations within the 2nd and 3rd quartiles of the
402 distribution. Unfortunately, subsequent measurements at the same target point were not provided. In
403 addition, during 2012 campaign, seabed sediments from a transect perpendicular to the shore, at 3, 6,
404 and 10 km from the river mouth respectively, have been excluded from the analysis due to their levels
405 of toxicity. The PE/003340/2012 sample shows the lowest amount of mud fraction compared to other
406 samples located at higher distance from the shoreline, but the highest concentration of Cu. By plotting
407 Cu concentrations *vs.* mud content (Fig. 2), it is straightforward that Cu amount in seabed samples
408 increases linearly with mud content, and the adjusted R-squared is higher than 0.85. The only point
409 falling outside this trend is PE/003340/2012. Unfortunately, mineralogical data of this sample are not
410 available. Nevertheless, it is highly probable that Cu concentration in sample PE/003340/2012 does not
411 belong to the main Cu distribution of our dataset, and thus it has to be considered as an outlier. As for
412 the other elements, the Cu distribution is better described using Tukey's boxplot and thus this statistical
413 approach has been preferred over adjusted boxplot.

414 Among the uncensored data, also Pb shows two extreme values according to the Tukey's boxplot. The
415 distributions of Pb and Cu concentrations in the dataset are similar, as for the multimodality and the
416 presence of extreme values at a certain distance from the rest of the data. In the case of lead, the
417 adjusted boxplot with inner fences as threshold values, includes additional measurements as probable
418 outliers toward higher values. Nevertheless, in analogy with the approach followed for Cu, only the two

419 extreme values of lead, as identified with the Tukey's boxplot, are marked as outliers. These samples
420 are identified as PE/005974/2016 and PE/005975/2016 (Table 1) and have been collected offshore
421 from Pineto town in the 2016 campaign. They belong to a transect perpendicular to the shore and with
422 intersection at the Calvano river mouth. Several samples within the transect have been collected at
423 about 0.5, 1 and 3 km away from the river mouth, during the 2015 and 2016 campaigns and all of them
424 have been classified as low toxicity sediments and thus included in the analysis. Within the transect, the
425 samples collected at higher distance from the river mouth show a progressive increase of Pb
426 concentrations with time. In particular, Pb concentration increase is higher than 50% from summer to
427 autumn sampling during the 2016 campaigns. This particular evidence should favour the hypothesis of
428 an exotic contamination. The same samples show the highest content of mud (Table 1), around 80%
429 and higher than 90% in PE/005974/2016 and PE/005975/2016, respectively, with about 13%
430 muscovite, and 7% chlorite and smectite, as shown in Table 2. Pb concentrations do not show clear
431 evidence of correlation with mud content in sediments (the adjusted R-squared is around 0.4), though it
432 is likely that the clay content may facilitate to the high Pb (and Cd) concentration observed in both
433 samples, due to its adsorption properties. Although further investigations are required in order to have
434 an understanding of the increasing concentrations with time and the anomalous values recorded in
435 2016, both measurements can be considered as outliers of Pb data distribution at this stage.

436 The remaining uncensored data include Ni, Cr and Zn concentrations in seabed sediments. The
437 distributions of the measurements relative to these elements are bi- or multimodal with no evidence of
438 anomalies (Fig. 4). The computation of the 90th percentile is carried out on the per-element dataset.

439 Censored data include concentrations of As, Cd, and Hg. The ROS method to generate summary
440 statistics and the boxplot graphical representation has been applied, as described in paragraph 2.2.5.

441 Concentrations below the instrumental detection limits are about 6%, 10% and 85% of the whole data

442 records, for As, Cd and Hg, respectively (Table 1). Their distributions show the proportion of censored
443 data as the part of the boxplot falling below the threshold line (Fig. 4). The lack of the lower whiskers
444 (Fig. 3) suggests that less than 25% of the data are censored observations. This is likely the case for As
445 and Cd. When almost all the boxplot disappears below the detection limit, as in the case of Hg (Fig. 4),
446 the 25th, 50th, and 75th percentiles have been estimated using the robust ROS method and drawn with
447 dashed lines.

448 Based on ROS, the distribution of As concentrations in the dataset shows two extreme values which are
449 not in spatial nor temporal relationships (Fig. 4). Sample PE/002536/2012 has been collected in 2012,
450 at about 6 km from the Vibrata river mouth, offshore Alba Adriatica town. Point PE/005830/2016 has
451 been sampled in 2016, near the Casalbordino shore. Target sample PE/002536/2012 belongs to a series
452 of four target points (from 0.5 up to 10 km distance) aligned along a transect perpendicular to the shore
453 and intersecting the shore at the Vibrata river mouth. The As concentration in the sample collected at
454 10 km from the shore ($11.0 \mu\text{g g}^{-1}$ d.m.) has not been included in the dataset due to the positive
455 response of the sample to ecotoxicological tests. Samples collected at 0.5 and 3 km from the shore have
456 been sampled every year from 2013 up to 2016. The sample at 3 km distance has been collected also in
457 2012. The whole sample set shows As concentrations within the 3rd quartile of the distribution (Fig. 4).
458 Sample PE/002536/2012 (As concentration of $24.0 \mu\text{g g}^{-1}$ d.m.) can indeed be considered as a real
459 anomaly within the whole and the local distribution. Sample PE/002536/2012 shows around 50% mud
460 content (Table 1), which is much higher than the mud amount measured in samples closest to the shore
461 within the same transect (variable from few percent up to about 30%). No mineralogical data are
462 available for sampling site of this transect, though the As concentration does not show any relationship
463 with the mud content in the data record. As a result, sample PE/002536/2012 can be considered as a
464 local contamination of unknown origin.

465 Sample PE/005830/2016 has been collected in October 2016. Before that survey, two additional
466 samples from the same target point has been collected in July 2016 (sample PE/004096/2016) and 2015
467 (sample PE/005844/2015) campaigns. All these samples have been included in the data record (Table
468 1), due to their low toxicity response. Samples PE/005844/2015 and PE/004096/2016 show As
469 concentration lower than $10 \mu\text{g g}^{-1}$ d.m., that is less than one third the concentration measured in
470 sample PE/005830/2016 ($34.0 \mu\text{g g}^{-1}$ d.m.). The unexpected and strong variation of As concentration in
471 samples PE/004096/2016 and PE/005830/2016, collected in July and October respectively of the same
472 year, suggests a potential contamination of anthropic origin.

473 The above considerations allow to consider samples PE/005830/2016 and PE/002536/2012 as outliers
474 of the As distribution. Therefore, the 90th percentile has been recalculated excluding the outliers.

475 With the 10% of censored data, the distribution of Cd concentrations, as computed with the ROS
476 method, shows six measurements falling outside the outer fences, and thus referable as probable
477 outliers (Fig. 4). All these samples have been collected in 2016, during two different surveys, carried
478 out in July and October. Samples PE/005974/2016 and PE/005975/2016, collected offshore from
479 Pineto, have been already discussed for Pb anomalies. The observation of anomalous levels of both Pb
480 and Cd in these sediments supports the interpretation of anthropic pollution. Given the closeness of a
481 gas field (Fig. 1), contamination from drilling operations cannot be excluded. Further investigations are
482 required in order to understand the nature and origin of this pollution, which is however out of the
483 purpose of the present study.

484 The samples with numbers PE/004098/2016, PE/005830/2016, PE/005831/2016 and PE/005832/2016,
485 have been collected in the near shore of Casalbordino. Samples PE/004098/2016 and PE/005832/2016
486 have been collected in July and October 2016, respectively. Within this group, sample PE/005830/2016

487 has already been discussed for showing an anomalous value of As, as well. Cd concentrations falling
488 within the 4th quartile of the distribution have been collected offshore of the Vibrata river and Pineto
489 town which are target sites already discussed for having high concentrations of certain elements in their
490 seabed sediments. Samples PE/004098/2016 up to PE/005832/2016 come from the closest sites to an
491 offshore gas field, called “Santo Stefano a Mare”. Therefore, it is not excluded that these sites are
492 experiencing an increment of pollution during the last years. Unfortunately, later measurements have
493 not been provided and in turn the trend of concentrations with time until today is not available.
494 Nevertheless, the measurements of these six samples have been considered as real outliers within
495 respective distributions based on the result of statistical analysis.

496 The distribution of Hg is for the most part estimated using ROS method, because censored
497 measurements are around 85% of the whole dataset. Detection limit of Hg measurements is $0.05 \mu\text{g g}^{-1}$
498 and the highest value of the data record is above $0.6 \mu\text{g g}^{-1}$ d.m. In this peculiar case, the ROS method
499 finds five suspicious measurements, all above $0.07 \mu\text{g g}^{-1}$ d.m. Only sample PE/001453/2014 has been
500 collected during 2014, near-shore of Pineto town. Samples PE/002533/2012, PE/002541/2012,
501 PE/003375/2012 and PE/003441/2012 have been collected in 2012 about 10 km offshore (Fig. 4h).
502 They are muddy sediments with mud content above 88% (Table 1). Unfortunately, there are no
503 subsequent measurements at the same sites. Sample PE/001453/2014 appears as a real anomaly of the
504 Hg distribution, especially due to its closeness to the shore. Due to the large number of censored data in
505 this distribution, and to the subsequent poor accuracy of the estimates, the 90th percentile has been
506 calculated including the whole measurements out of sample PE/001453/2014, which is very suspicious
507 of being contaminated.

508 To account for eventual patterns in the dataset and to improve the determination of the local natural
509 background of metal concentrations, multivariate statistics was also employed. PCA was carried out

510 using 90 samples and 7 variables (mud fraction, As, Cd, Cu, Cr, Ni, and Pb concentrations). The results
511 are shown in Figure 5. The first four principal components (PCs) explain more than 96% of the total
512 variance within the dataset, with the following proportions: 59.9% (PC1), 15.0% (PC2), 13.4% (PC3),
513 and 8.3% (PC4). Principal component loadings (listed in the table in Figure 5 and represented as arrows
514 in the plot of the variances associated with the PCs) reveal how the original variables influence the
515 principal components. As the results show, the first PC which explains the largest variance in the data,
516 is mainly controlled by Ni, Cr and mud content, with positive loadings. Ni and Cr have strong positive
517 correlations with the mud fraction in samples, as already shown in Figure 2. Univariate statistics has
518 not detected any outlier for both distributions. In addition, the highest concentrations of Ni and Cr
519 measured in this study (58.8 and 88.0 $\mu\text{g g}^{-1}$ d.m., respectively) are in accordance with or even lower
520 than the values measured in the four samples considered here from Spagnoli et al. (2014) and shown in
521 Figure 1 (62 and 112 $\mu\text{g g}^{-1}$ on average, respectively).

522 Lead is also relevant for PC1, although it has a strong influence on PC2. Univariate statistics has led to
523 the identification of two possible outliers in the distribution of Pb concentrations. These two extreme
524 values plot in the upper right portion of the PC1 and PC2 domain (Fig. 5), together with samples
525 characterized by high concentrations of Pb and Cd and marked as outliers with respect to the
526 distributions of these elements. According to Spagnoli et al. (2014), Pb concentrations higher than 30
527 $\mu\text{g g}^{-1}$ d.m. (Table 1) are about double the concentrations they measured at greater distance from the
528 shoreline, thus reinforcing the hypothesis that these values are to be considered as anomalies.

529 Cu, which also shows positive correlation with the mud fraction in sediments (Fig. 2), mainly
530 influences PC4 with a strong positive loading in a component which has a little effect on the total
531 variation. It is likely that the only anomaly in the distribution of Cu concentrations within the dataset

532 (78.4 $\mu\text{g g}^{-1}$ d.m., higher than double the maximum concentration measured by Spagnoli et al. (2014)),
533 as detected with the boxplot method, is strongly responsible for this behaviour.

534 The variance domain explained with PC1 and PC2 also allows a cluster of samples in the lower right
535 portion of the plot to be identified. All those samples are suspected outliers based on univariate
536 statistics of Hg concentrations. However, since Hg has not been included as a variable in the principal
537 component analysis and in turn its influence on the total variation of data cannot be estimated with
538 PCA results, for this group of samples, and those in their closeness, the variable mostly affecting the
539 total variation is the mud fraction. Therefore, the large amount of mud in these samples is likely to
540 drive the Hg enrichment. In addition, trace metals concentrations of these samples locate in the 4th
541 quartile space for As, Cu, Cr, Ni, and Pb, thus supporting the hypothesis of a natural enrichment.

542 As and Cu control PC3 and PC4, respectively. The variance domain explained by both PCs shows a
543 small spread around the two components, except for a few points which have been identified as outliers
544 with the boxplot method.

545 The PCA results also show a very homogeneous dataset with the occurrence of few anomalies,
546 according to the boxplot method. In addition, there is no evidence of a different behaviour between
547 seabed sediments collected to the N and to the S of the Pescara river mouth (Fig. 5). Indeed, PCA
548 results confirm the main influence of grain size on the total variance of data, with random occurrences
549 of anomalous metal concentrations, apparently not related to natural processes and in turn not suitable
550 for determination of local background concentration.

551 Table 3 lists the lower and upper limits (L_1 and L_2 , respectively) of trace metals content, as established
552 with the regulation n. 173/2016, together with the lower local limits, as calculated in this study. Based
553 on the procedure described in the Regulation n. 173/2016, L_{loc} was computed including all the

554 measurements in the computation. By removing the extreme values as outliers, L^*_{1loc} was computed.
555 The results differ only for few decimals, thus proving that the integrated approach using chemical and
556 ecotoxicological analyses is very effective. By comparing our results with the local background
557 estimated at the national level (decree n.173/2016), only lower values for Hg, Pb, Cu and Zn, and upper
558 values for Cr and Ni, were observed. This is not surprising since the Adriatic seabed sediments receive
559 much of their input from the Po river, which drains ophiolitic complexes occurring in the Alpine sector
560 (Spagnoli et al., 2014).

561

562 **Conclusions**

563 The first attempt to measure the local background levels of heavy metals in Adriatic seabed sediments
564 in front of the Abruzzo region coastline has been accomplished. The estimation of this background
565 level is requested by law (decree n.173/2016) to determine the “natural” characterization of marine
566 sediments. Several sampling campaigns have been carried out by the regional agency ARTA with
567 different objectives between 2011 and 2016. According to the national regulation, ecotoxicological
568 tests aiming at assessing the bioavailability of the pollutants in sediments have been used to subset the
569 data record. The chemical and mineralogical composition of the 110 samples with negative response to
570 the ecotoxicological tests have been used for the determination of the background levels. Both
571 univariate (Tukey's box plot) and multivariate statistics (PCA) were used to understand data structure
572 and distribution and identify probable outliers. The values of the 90th percentile of the statistical
573 distribution were considered to identify the local background L_{1loc} according to the mentioned national
574 law. Further calculation of the local background (L^*_{1loc}) has been performed after outliers removal.
575 However, any significant differences between the two approaches were not observed.

576 A few outliers have been identified with anomalous contents of trace elements which suggest a
577 potential anthropic contamination and may deserve further investigation.

578

579 **Conflict of interest statement**

580 The authors declare no conflicts of interest.

581 **Acknowledgements**

582 The authors thank the G. d'Annunzio University of Chieti-Pescara and the Italian Ministry of
583 Education, University and Research for financial support. The authors also wish to thank two
584 anonymous reviewers for having strongly improved the manuscript.

585

586 **References**

587 APAT-ICRAM, 2007. Manuale per la movimentazione di sedimenti marini.
588 [http://www.isprambiente.gov.it/en/publications/handbooks-and-guidelines/manuale-per-la-
589 movimentazione-di-sedimenti-marini-1](http://www.isprambiente.gov.it/en/publications/handbooks-and-guidelines/manuale-per-la-
589 movimentazione-di-sedimenti-marini-1)

590 ASTM E724 - 98, 2012. Standard guide for conducting static acute toxicity tests starting with
591 embryos of four species of saltwater bivalve molluscs.

592 Abraham, G.M.S., Parker, R.J., 2008. Assessment of heavy metal enrichment factors and the degree
593 of contamination in marine sediments from Tamaki Estuary, Auckland, New Zealand. Environ. Monit.
594 Assess. 136, 227-238.

595 Amorosi, A., Maselli, V., Trincardi, F., 2016. Onshore to offshore anatomy of a late Quaternary
596 source-to-sink system (Po plain – Adriatic Sea, Italy). Earth Sci. Rev. 153, 212-237.

597 Bábek, O., Matys Grygar, T., Faměra, M., Hron, K., Nováková, T., Sedláček, J., 2015. Geochemical
598 background in polluted river sediments: how to separate the effects of sediment provenance and grain
599 size with statistical rigour? *Catena* 135, 240-253.

600 Birch, G.F., 2017. Determination of sediment metal background concentrations and enrichment in
601 marine environments – A critical review. *Sci. Total Environ.* 580, 813-831.

602 Carpenter, A., Lozano, R., Sammalisto, K., Astner, L., 2018. Securing a port's future through
603 circular economy: experiences from the Port of Gävle in contributing to sustainability. *Mar. Pollut.*
604 *Bull.* 128, 539–547.

605 Cattaneo, A., Correggiari, A., Langone, L., Trincardi, F., 2003. The late-Holocene Gargano
606 subaqueous delta, Adriatic shelf: sediment pathways and supply fluctuations. *Mar. Geol.* 193, 61-91.

607 Cortecchi, G., Dinelli, E., Boschetti, T., Arbizzani, P., Pompilio, L., Mussi, M., 2008. The Serchio
608 River catchment, northern Tuscany: Geochemistry of stream waters and sediments, and isotopic
609 composition of dissolved sulfate. *Appl. Geochem.* 23, 1513-1543.

610 Covelli, S., Fontolan, G., 1997. Application of a normalization procedure in determining regional
611 geochemical baselines. *Environ. Geol.* 30, 1-2, 34-45.

612 Decree 15th July 2016 n. 173, 2016. Regolamento recante modalità e criteri tecnici per
613 l'autorizzazione all'immersione in mare dei materiali di escavo di fondali marini. 16G00184 (GU Serie
614 Generale n. 208 del 06/09/2016 – Suppl. Ordinario n. 40).
615 <http://www.gazzettaufficiale.it/eli/id/2016/09/06/16G00184/sg>

616 De Lazzari, A., Rampazzo, G., Pavoni, B., 2004. Geochemistry of sediments in the Northern and
617 Central Adriatic Sea. *Estuar. Coast. Shelf S.* 59, 429-440.

618 Dinelli, E., Lucchini, F., 1999. Sediment supply to the Adriatic Sea basin from the Italian rivers:
619 geochemical features and environmental constraints, *Giornale di Geologia*, ser. 3, 61, 121-132.

620 Dinwoodie, J., Tuck, S., Knowles, H., Benhin, J., Sansom, M., 2012. Sustainable development of
621 maritime operations in ports. *Bus. Strat. Env.* 21, 111–126.

622 Felja, I., Romić, M., Romić, D., Bakić, H., Pikelj, K., Juračić, M., 2016. Application of empirical
623 model to predict background metal concentration in mixed carbonate-alumosilicate sediment (Adriatic
624 Sea, Croatia). *Mar. Pollut. Bull.* 106, 190-199.

625 Frignani, M., Langone, L., Ravaioli, M., Sorgente, D., Alvisi, F., Albertazzi, S., 2005. Fine-
626 sediment mass balance in the Western Adriatic continental shelf over a century time scale. *Mar. Geol.*
627 222-223, 113-133.

628 Goudeau, M.L.S., Grauel, A.L., Bernasconi, S.M., de Lange, G.J., 2013. Provenance of surface
629 sediments along the southeastern Adriatic coast off Italy: an overview. *Estuar. Coast. Shelf S.* 134, 45-
630 56.

631 Hamilton, M.A., Russo R.C. Thurston R.V., 1978. Trimmed Spearman-Kärber method for
632 estimating median lethal concentrations in toxicity bioassays. *Environ. Sci. Technol.* 12, 714 -720.

633 Harris, C.K., Sherwood, C.R., Signell, R.P., Bever, A.J., Warner, J.C., 2008. Sediment dispersal in
634 the northwestern Adriatic Sea. *J. Geophys. Res.* 113, C11S03.

635 Heimbürger, L.E., Cossa, D., Thibodeau, B., Khripounoff, Al., Mas, V., Chiffoleau, J.F., Schmidt,
636 S., Migon, C., 2012. Natural and anthropogenic trace metals in sediments of the Ligurian Sea
637 (Northwestern Mediterranean). *Chem. Geol.* 291, 141-151.

638 Helsel, D.R., 2012. Statistics for censored environmental data using Minitab and R. John Wiley and
639 Sons, Hoboken, NJ.

640 Helsel, D.R., 2005. Nondetects and data analysis. John Wiley and Sons, New York.

641 Helsel, D.R., Cohn, T.A., 1988. Estimation of descriptive statistics for multiply censored water
642 quality data. Water Resour. Res. 24, 1997-2004.

643 Hubert, M., Vandervieren, E., 2008. An adjusted boxplot for skewed distributions. Comput. Stat.
644 Data Anal. 52, 5186-5201.

645 ICRAM, 2001. Programma di monitoraggio per il controllo dell'ambiente marino-costiero (triennio
646 2001-2003). Metodologie analitiche di riferimento.
647 [http://www.isprambiente.gov.it/it/pubblicazioni/manuali-e-linee-guida/metodologie-analitiche-di-](http://www.isprambiente.gov.it/it/pubblicazioni/manuali-e-linee-guida/metodologie-analitiche-di-riferimento-del)
648 [riferimento-del](http://www.isprambiente.gov.it/it/pubblicazioni/manuali-e-linee-guida/metodologie-analitiche-di-riferimento-del)

649 Ilijanić, N., Miko, S., Petrinec, B., Franić, Z., 2014. Metal deposition in deep sediments from the
650 Central and South Adriatic Sea. Geologia Croatica 67/3, 185-205.

651 ISO 11465, 1993. Soil quality - Determination of dry matter and water content on a mass basis -
652 Gravimetric method.

653 ISO 10253, 2016. Water quality - Marine algal growth inhibition test with *Skeletonema sp.* and
654 *Phaeodactylum tricornutum*.

655 Langone, L., Conese, I., Miserocchi, S., Boldrin, A., Bonaldo, D., Carniel, S., Chiggiato, J.,
656 Turchetto, M., Borghini, M., Tesi, T., 2016. Dynamics of particles along the western margin of the
657 Southern Adriatic: processes involved in transferring particulate matter to the deep basin. Mar. Geol.
658 375, 28-43.

659 Lee, L., Helsel, D.R., 2005. Statistical analysis of water-quality data containing multiple detection
660 limits: S-language software for regression on order statistics. *Computers and Geosciences* 31, 1241-
661 1248.

662 Libralato, G., Avezzù, F., Volpi Ghirardini, A., 2011. Lignin and tannin toxicity to *Phaeodactylum*
663 *tricornutum* (Bohlin). *J. Hazard. Mater.* 194, 435–439.

664 Lopes-Rocha, M., Langone, L., Miserocchi, S., Giordano, P., Guerra, R., 2017a. Spatial patterns and
665 temporal trends of trace metal mass budgets in the Western Adriatic sediments (Mediterranean Sea).
666 *Sci. Total Environ.* 599-600, 1022-1033.

667 Lopes-Rocha, M., Langone, L., Miserocchi, S., Giordano, P., Guerra, R., 2017b. Detecting long-
668 term temporal trends in sediment-bound metals in the western Adriatic (Mediterranean Sea). *Mar.*
669 *Pollut. Bull.* 124, 270-285.

670 Mali, M., Dell'Anna, M.M, Mastroilli, P., Damiani, L., Ungaro, N., Belviso, C., Fiore, S., 2015.
671 Are conventional statistical techniques exhaustive for defining metal background concentrations in
672 harbour sediments? A case study: The Coastal Area of Bari (Southeast Italy). *Chemosphere* 138, 708-
673 717.

674 Matschullat, J., Ottenstein, R., Reimann, C., 2000. Geochemical background – can we calculate it?
675 *Environ. Geol.* 39, 990-1000.

676 Matys Grygar, T., Popelka, J., 2016. Revisiting geochemical methods of distinguishing natural
677 concentrations and pollution by risk elements in fluvial sediments. *J. Geochem. Explor.* 160, 39-57.

678 Migani, F., Borghesi, F., Dinelli, E., 2015. Geochemical characterization of surface sediments from
679 the northern Adriatic wetlands around the Po river delta. Part I: bulk composition and relation to local
680 background. *J. Geochem. Explor.* 156, 72-88.

681 Moore, D.M., Reynolds Jr., R.C., 1997. X-ray diffraction and the identification and analysis of clay
682 minerals, 2nd ed., Oxford University Press, Oxford, UK.

683 Onorati, F., Volpi Ghirardini, A., 2001. Informazioni fornite dalle diverse matrici da testare con i
684 saggi biologici: applicabilità di *Vibrio fischeri*. *Biol. Mar. Medit.* 8, 31-40.

685 Natali, C., Bianchini, G., 2018. Natural vs anthropogenic components in sediments from the Po river
686 delta coastal lagoons (NE Italy). *Environ. Sci. Pollut. Res.* 25, 2981-2991.

687 Picone, M., Bergamin, M., Losso, C., Delaney, E., Arizzi Novelli, A., Volpi Ghirardini, A., 2016.
688 Assessment of sediment toxicity in the Lagoon of Venice (Italy) using a multi-species set of bioassays.
689 *Ecotox. Environ. Safe.* 123, 32-44.

690 Piva, F., Ciaprini, F., Onorati, F., Benedetti, M., Fattorini, D., Ausili, A., Regoli, F., 2011. Assessing
691 sediment hazard through a weight of evidence approach with bioindicator organisms: a practical model
692 to elaborate data from sediment chemistry, bioavailability, biomarkers and ecotoxicologically
693 bioassays. *Chemosphere* 83, 475-485.

694 R Core Team, 2018. R: A language and environment for statistical computing. R Foundation for
695 Statistical Computing, Vienna, Austria. URL <https://www.R-project.org/>.

696 Reimann, C., Garrett, R.G., 2005. Geochemical background – concept and reality. *Sci. Total*
697 *Environ.* 350, 12-27.

698 Rodríguez, J.G., Tueros, I., Belzunce, M.J., France, J., Solaun, O., Valencia, V., Zuazo, A., 2006.
699 Maximum likelihood mixture estimation to determine metal background values in estuarine and coastal
700 sediments within the European Water Framework Directive. *Sci. Total Environ.* 370, 278-293.

701 Romano, S., Langone, L., Frignani, M., Albertazzi, S., Focaccia, P., Bellucci, L.G., Ravaioli, M.,
702 2013. Historical pattern and mass balance of trace metals in sediments of the northwestern Adriatic Sea
703 Shelf. *Mar. Pollut. Bull.* 76, 32-41.

704 Spagnoli, F., Dinelli, E., Giordano, P., Marcaccio, M., Zaffagnini, F., Frascari, F., 2014.
705 Sedimentological, biogeochemical and mineralogical facies of Northern and Central Western Adriatic
706 Sea. *J. Mar. Syst.* 139, 183-203.

707 Stanimirova, I., 2013. Practical approaches to principal component analysis for simultaneously
708 dealing with missing and censored elements in chemical data. *Analytica Chimica Acta*, 796, 27-37.

709 Tukey, J.W., 1977. *Exploratory data analysis*. Addison-Wesley, Reading, Massachusetts, 39-49.

710 UNI EN ISO 11348-3, 2009. Qualità dell'acqua - Determinazione dell'effetto inibitorio di campioni
711 acquosi sull'emissione di luce di *Vibrio fischeri* (prova su batteri luminescenti) - Parte 3: Metodo con
712 batteri liofilizzati.

713 UNI EN ISO 11885, 2009. Qualità dell'acqua - Determinazione di alcuni elementi mediante
714 spettrometria di emissione ottica al plasma accoppiato induttivamente.

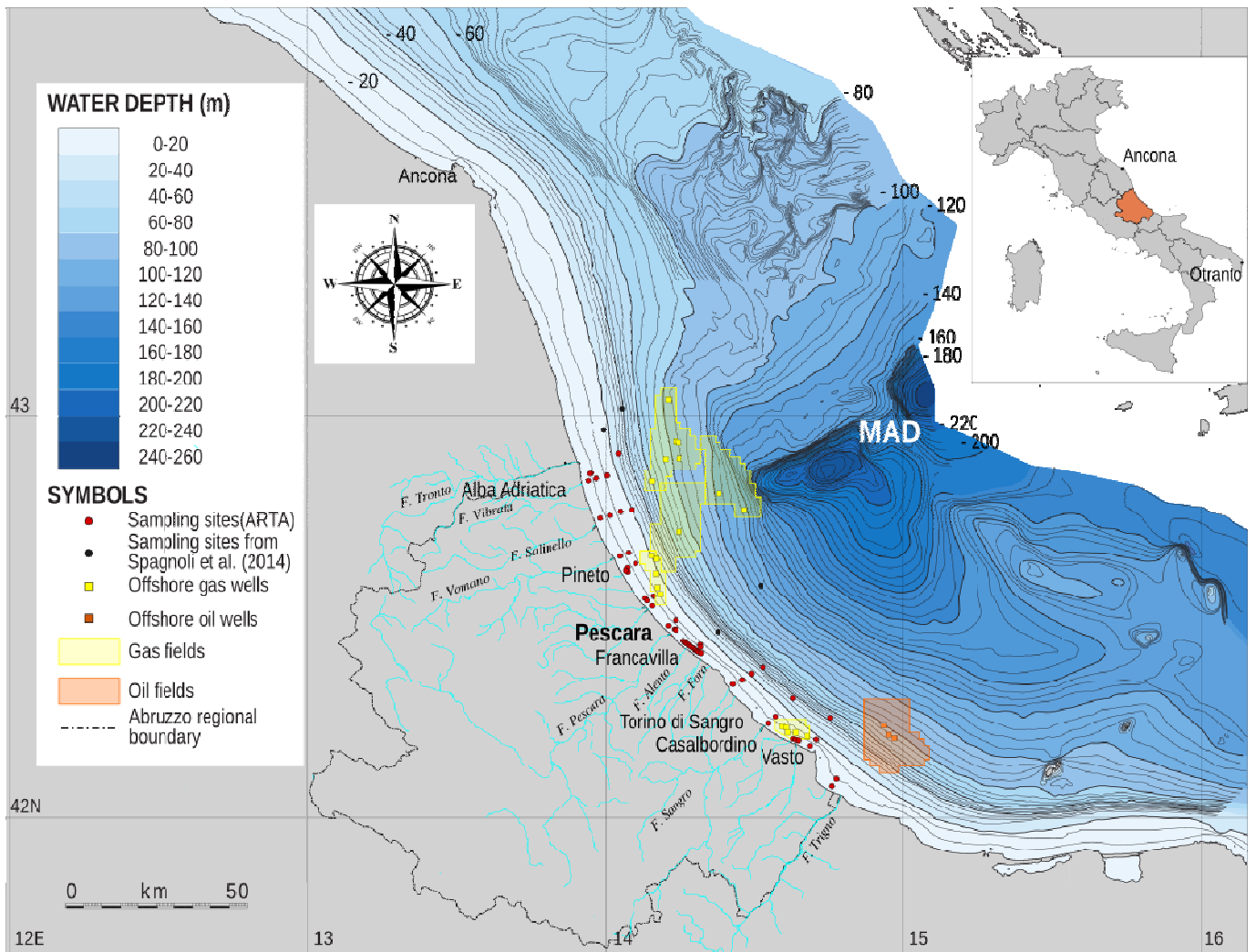
715 UNI EN 15936:2012. Fanghi, rifiuti organici trattati e suolo - Determinazione del carbonio organico
716 totale (TOC) mediante combustione secca.

717 US EPA, 1991. Evaluation of dredged material proposed for ocean disposal. *Testing Manual*
718 USEPA-503-8-90/002.

719 US EPA 7471B, 2007. Mercury in solid or semisolid waste (manual cold-vapor), part of test
720 methods for evaluating solid waste, physical/chemical methods.

721 Volpi Ghirardini, A., Losso, C., Arizzi Novelli, A., Baù, A., Edouard, H., Ghetti, P.F., 2005. *Mytilus*
722 *galloprovincialis* as bioindicator in embryotoxicity testing to evaluate sediment quality in the lagoon of
723 Venice (Italy) *Chem. Ecol.* 21, 455-463

724 Weltje, G.J., Brommer, M.B., 2011. Sediment-budget modelling of multi-sourced basin fills:
725 application to recent deposits of the Western Adriatic mud wedge (Italy). *Basin Res.* 23, 291-308.

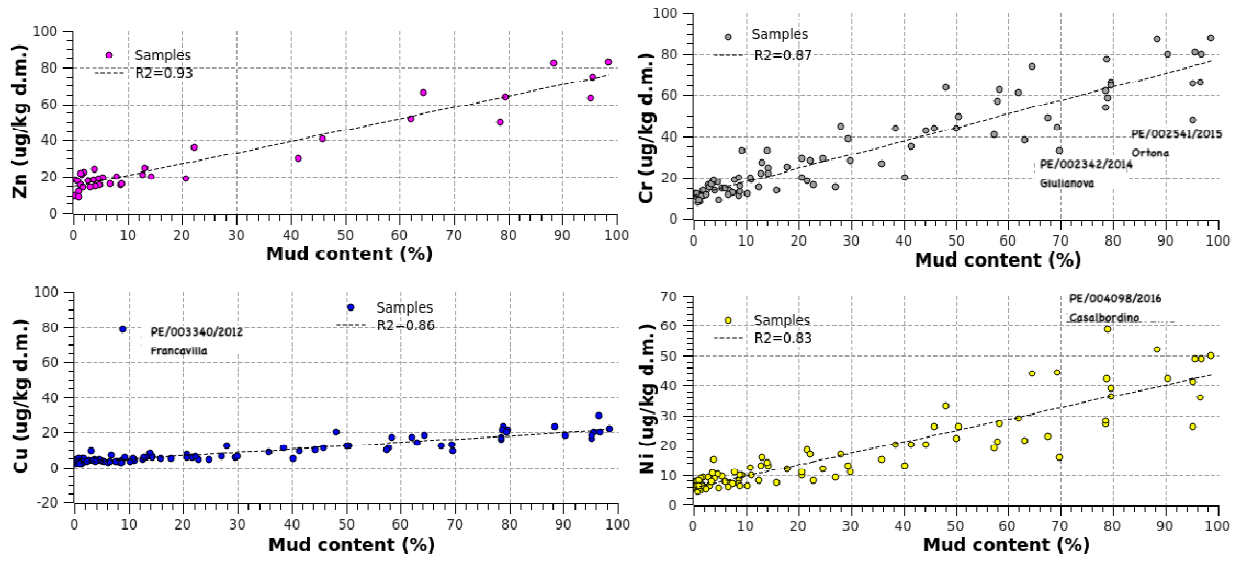


726

727 **Fig. 1.** Map of the study area showing the locations of the sediment sampling stations relevant for this study (red
 728 circles) and from the work of Spagnoli et al. (2014) (black circles). The offshore gas and oil wells (yellow and
 729 orange squares, respectively) occurring in the region are also shown. Bathymetry of the western Adriatic sea (5
 730 m contour lines), is from Cattaneo et al. (2003).

731

732

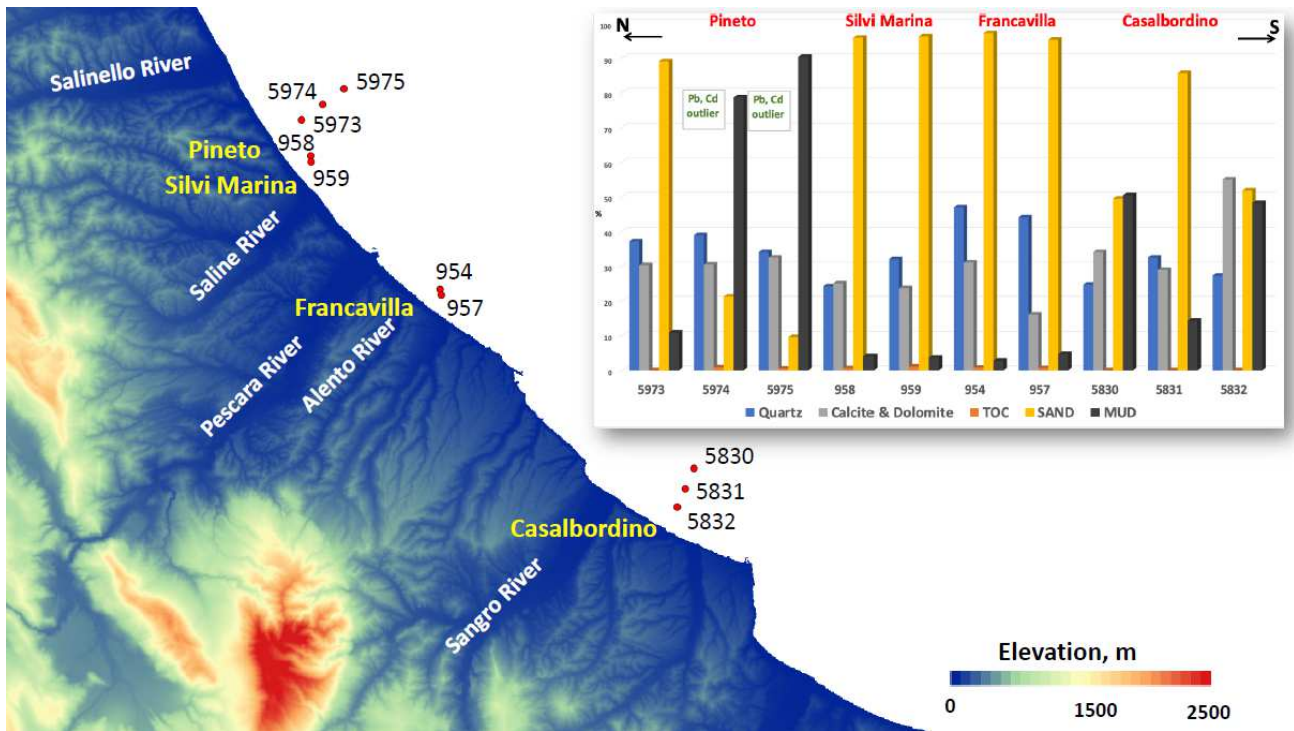


733

734 **Fig. 2.** Variation of the trace element with mud content.

735

736



737

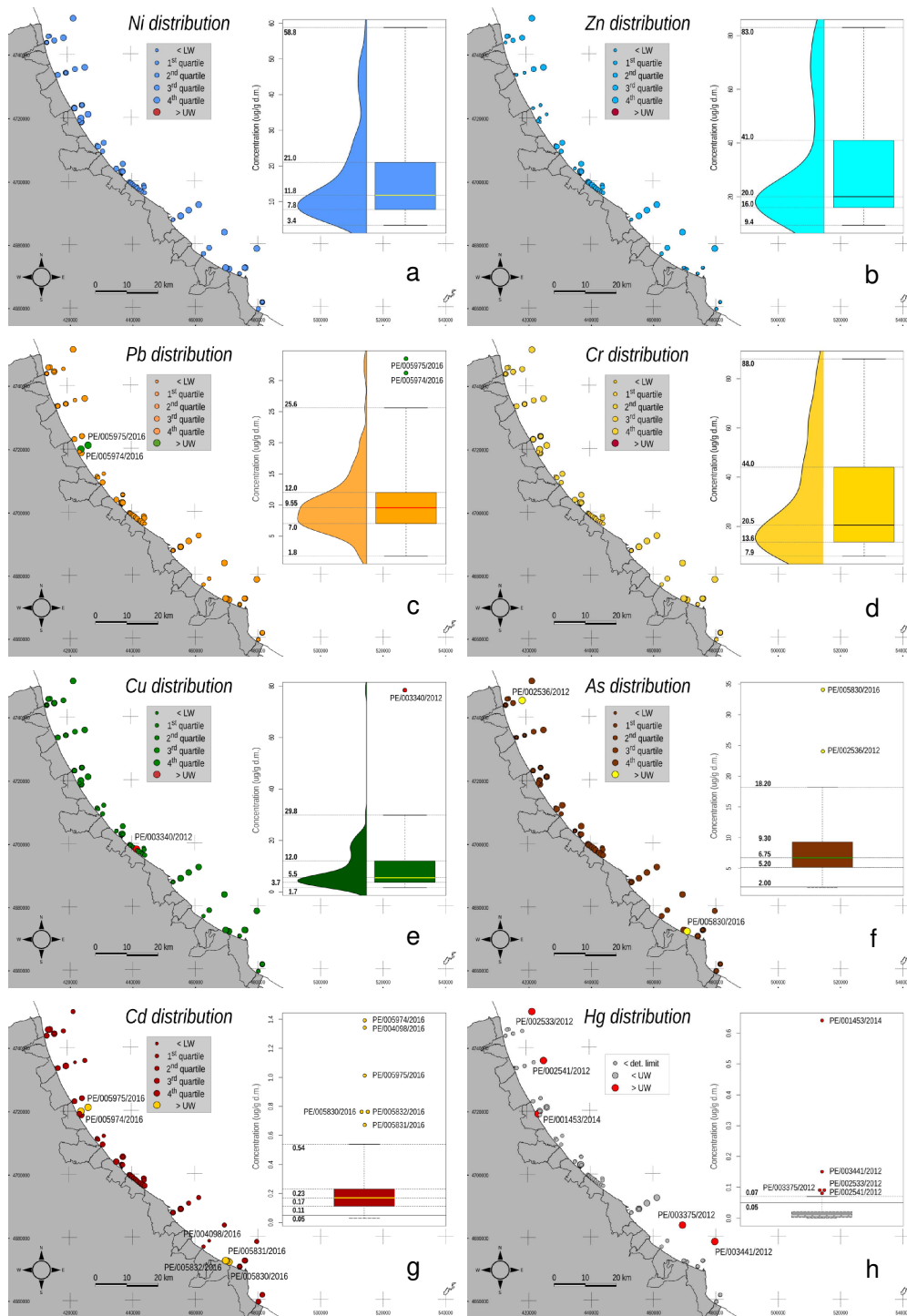
738

739 **Fig. 3.** Comparison of the abundance (as wt%) of the main mineralogical species (Quartz and Ca,Mg-
740 Carbonates), total organic content (TOC) and granulometry of selected samples collected during the 2016
741 campaign. The corresponding values are available in Table 1 and 2 (the samples name prefix PE/00 ... and the
742 suffix .../2016 have been removed in the map). The position of the sampling sites is provided in the map.

743

744

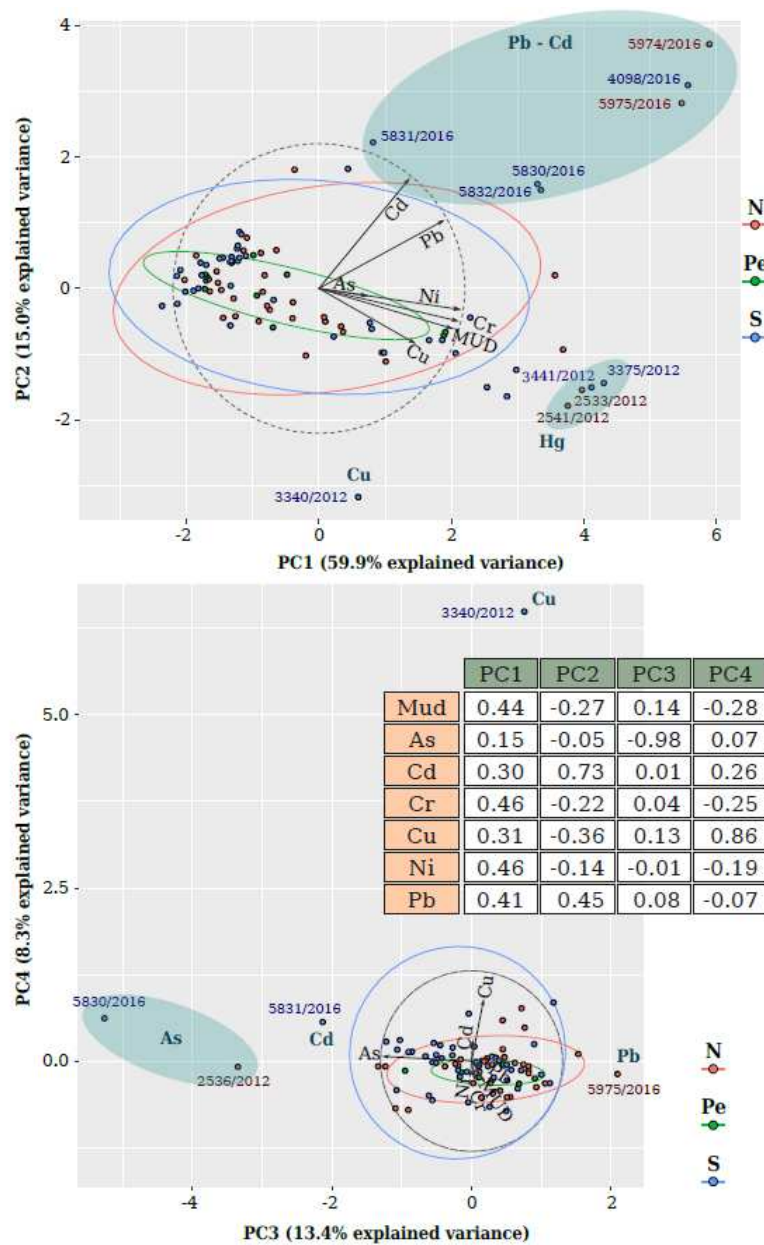
745



746

747 **Fig. 4.** Charts of statistical and geographical distribution of trace elements. The circles on maps have variable
 748 size, depending on the position within the Tukey's boxplot on the right; density plots and the concentrations (as

749 $\mu\text{g g}^{-1}$ of dry matter) of relevant percentiles are also shown. Identified outliers are displayed in different colors
750 with their label and year of sampling campaign.



752

753 **Fig. 5.** Bidimensional plots of the total variance explained with the four main principal components, as results
 754 from PCA. The score of each sample is plotted with circles having different colours, according to the main
 755 geographical sector of sample provenance (to the North (N) and South (S) of the Pescara river (Pe) mouth).The
 756 directions of the arrows show the relative loadings of each variable on each pair of PCs. The loadings are also
 757 listed in the table per variable. The sample points with the name highlighted have been recognized as extreme

758 values with univariate statistics for the concentration of the indicated elements. The prefix PE/00 ... has been
759 omitted from the name for clarity. The ellipses enclose data points with similar behavior.

760

761

762 **Table 1**

763 Concentration of trace metals and granulometry of the 110 samples analysed in this study with geographical
 764 indication of the sampling area (see also Fig. 1 and 2). Chemical content is expressed as $\mu\text{g g}^{-1}$ of dry matter.
 765 Grain size fractions are expressed as wt%.

766 Bold values correspond to outliers, as resulted from the statistical analysis.

767

768

Label	Nearby town	Metal content ($\mu\text{g/g d.m.}$)								Gravel	Sand	Mud
		As	Cd	Cr	Cu	Hg	Ni	Pb	Zn	wt%	wt%	wt%
<i>Detection limits</i>	-	<2.0	<0.05	<1.0	<1.0	<0.05	<2.0	<2.0	<1.0	-	-	-
PE/005831/2015	Pineto	6.2	0.34	64.9	15.5	<0.05	46.6	12.7	NA	NA	NA	NA
PE/005832/2015	Pineto	4.7	0.35	53.2	13.8	<0.05	28.8	16.5	NA	NA	NA	NA
PE/005833/2015	Pineto	12.8	0.44	21.3	6.3	<0.05	11.6	12.3	NA	NA	NA	NA
PE/005842/2015	Casalbordino	8.5	0.29	20.5	5.1	<0.05	11.6	10.5	NA	NA	NA	NA
PE/005843/2015	Casalbordino	5.6	0.25	26.9	7.4	<0.05	14.6	7.5	NA	NA	NA	NA
PE/005844/2015	Casalbordino	6.8	0.23	20.5	4.5	<0.05	12.9	13.1	NA	NA	NA	NA
PE/003578/2016	Pineto	9.4	0.18	18.7	4.0	<0.05	10.0	11.3	NA	0.0	88.9	11.1
PE/003579/2016	Pineto	9.7	0.45	66.2	21.0	<0.05	36.4	20.9	NA	0.9	19.5	79.6
PE/003580/2016	Pineto	8.3	0.26	66.3	29.8	<0.05	35.9	19.6	NA	0.0	3.5	96.5
PE/004096/2016	Casalbordino	9.9	0.23	44.4	12.8	<0.05	44.4	14.9	NA	0.0	30.6	69.4
PE/004097/2016	Casalbordino	9.6	0.54	18.2	5.7	<0.05	18.2	16.5	NA	0.0	78.4	21.6
PE/004098/2016	Casalbordino	6.1	1.34	58.8	22.8	<0.05	58.8	25.6	NA	0.0	21.0	79.0
PE/005830/2016	Casalbordino	34.0	0.76	49.7	12.4	<0.05	26.1	19.4	NA	0.0	49.5	50.5
PE/005831/2016	Casalbordino	18.2	0.67	24.7	6.2	<0.05	12.9	17.3	NA	0.0	85.7	14.3
PE/005832/2016	Casalbordino	10.6	0.76	64.0	20.0	<0.05	33.0	21.0	NA	0.0	51.9	48.1
PE/005973/2016	Pineto	<2.0	0.48	19.8	4.8	<0.05	12.2	15.4	NA	0.0	89.1	10.9
PE/005974/2016	Pineto	8.7	1.39	77.8	21.3	0.07	42.3	31.2	NA	0.0	21.3	78.7
PE/005975/2016	Pineto	2.5	1.01	79.9	18.0	0.06	42.2	33.5	NA	0.0	9.6	90.4
PE/001453/2014	Pineto	5.9	0.21	12.0	2.1	0.64	5.8	5.9	9.9	2.8	97.0	0.2
PE/000059/2015	Pescara	7.0	0.19	54.0	16.0	0.06	27.0	14.0	50.0	4.5	16.9	78.6
PE/000060/2015	Pescara	5.8	0.17	61.0	17.0	0.06	29.0	15.0	52.0	22.4	15.6	62.0
PE/000061/2015	Pescara	8.2	0.16	19.0	3.3	<0.05	11.0	11.0	20.0	0.0	92.1	7.9
PE/006174/2015	Francavilla	10.3	0.20	13.6	3.3	<0.05	9.2	9.5	22.2	0.0	98.1	1.9
PE/006175/2015	Francavilla	9.3	0.18	11.1	4.7	<0.05	7.8	8.4	18.4	1.7	97.9	0.4
PE/006176/2015	Francavilla	11.2	0.16	11.0	3.9	<0.05	8.7	9.4	21.4	0.0	98.5	1.5
PE/006177/2015	Francavilla	9.3	0.18	12.9	3.7	<0.05	8.6	8.2	15.7	0.0	91.3	8.7
PE/006179/2015	Francavilla	13.0	0.15	11.1	5.3	<0.05	7.8	9.8	21.9	0.0	98.7	1.3
PE/006180/2015	Francavilla	12.0	0.17	10.9	5.2	<0.05	7.7	8.6	17.9	0.4	98.9	0.7
PE/006181/2015	Francavilla	9.7	0.16	14.6	3.4	<0.05	9.5	9.8	19.5	0.0	94.5	5.5

PE/006182/2015	Francavilla	3.2	0.16	13.6	6.6	<0.05	7.1	5.8	16.1	24.3	68.9	6.8
PE/006195/2015	Francavilla	11.5	0.22	11.0	3.0	<0.05	6.7	11.2	15.4	0.0	98.7	1.3
PE/006196/2015	Francavilla	10.0	0.21	11.0	4.9	<0.05	6.2	11.8	14.6	0.7	97.5	1.8
PE/006197/2015	Francavilla	6.9	0.21	9.1	3.9	<0.05	5.5	5.6	15.6	12.9	82.3	4.8
PE/000954/2016	Francavilla	6.7	0.20	16.3	3.7	<0.05	9.3	10.2	17.7	0.0	97.2	2.8
PE/000957/2016	Francavilla	7.2	0.16	17.7	4.5	<0.05	10.3	10.7	18.7	0.0	95.3	4.7
PE/000958/2016	Silvi Marina	6.4	0.13	13.6	3.9	<0.05	8.8	7.8	14.9	0.0	95.9	4.1
PE/000959/2016	Silvi Marina	6.5	0.19	17.4	4.3	<0.05	10.5	10.3	18.4	0.0	96.3	3.7
PE/003461/2016	Martinsicuro	5.7	0.28	15.4	9.0	<0.05	6.2	10.5	14.2	0.0	96.9	3.1
PE/003462/2016	Martinsicuro	6.0	0.26	19.7	7.5	<0.05	10.0	11.1	18.7	0.0	79.3	20.7
PE/004439/2013	Pescara	5.8	<0.05	15.0	2.4	<0.05	7.9	7.7	NA	0	93.9	6.1
PE/004440/2013	Pescara	7.2	0.09	25.0	5.1	<0.05	12.0	8.6	NA	0	82.2	17.8
PE/004441/2013	Pineto	6.8	0.10	49.0	12.0	<0.05	23.0	10.0	NA	0	32.4	67.6
PE/004578/2013	Pineto	6.9	0.06	43.0	10.0	<0.05	20.0	11.0	NA	0	55.7	44.3
PE/004579/2013	Giulianova	5.8	<0.05	20.0	4.8	<0.05	13.0	9.7	NA	0	59.8	40.2
PE/004580/2013	Giulianova	6.5	<0.05	29.0	4.7	<0.05	12.0	9.8	NA	0	75.3	24.7
PE/004581/2013	A. Adriatica	6.1	<0.05	20.0	2.9	<0.05	8.2	8.7	NA	0	91.4	8.6
PE/004582/2013	A. Adriatica	7.5	<0.05	39.0	5.8	<0.05	13.0	9.9	NA	0	70.5	29.5
PE/004583/2013	Ortona	5.7	<0.05	11.0	2.4	<0.05	6.9	7.5	NA	0	91.3	8.7
PE/004584/2013	Ortona	7.2	0.14	62.0	17.0	0.06	28.0	14.0	NA	0	21.4	78.6
PE/004664/2013	Vasto	5.9	<0.05	11.0	3.1	<0.05	6.0	6.3	NA	0	99	1
PE/004665/2013	San Salvo	7.9	<0.05	11.0	3.0	<0.05	6.3	6.8	NA	0	98.3	1.7
PE/004666/2013	San Salvo	6.3	0.07	44.0	11.0	<0.05	20.0	9.6	NA	0	61.6	38.4
PE/004667/2013	Vasto	8.1	<0.05	57.0	11.0	<0.05	21.0	12.0	NA	0	42.1	57.9
PE/002342/2014	Giulianova	4.0	0.26	33.0	9.1	<0.05	16.0	5.6	NA	0.0	30.3	69.7
PE/002344/2014	A. Adriatica	7.2	0.17	29.0	5.5	<0.05	11.0	7.1	NA	0.0	79.3	20.7
PE/002345/2014	A. Adriatica	8.3	0.23	33.0	5.8	<0.05	9.9	7.4	NA	0.0	90.7	9.3
PE/002378/2014	Vasto	12.0	0.18	12.0	3.2	<0.05	5.9	7.8	NA	0.0	99.7	0.3
PE/002379/2014	Vasto	9.3	0.19	44.0	12.0	<0.05	22.0	10.0	NA	0.0	50.0	50.0
PE/002380/2014	San Salvo	8.3	0.16	12.0	3.1	<0.05	6.3	6.9	NA	0.0	99.3	0.7
PE/002381/2014	San Salvo	7.7	0.15	28.0	6.3	<0.05	11.0	7.6	NA	0.0	70.1	29.9
PE/002388/2014	Ortona	9.6	0.19	17.0	3.9	<0.05	7.6	8.1	NA	0.0	96.6	3.4
PE/002389/2014	Ortona	5.2	0.17	63.0	17.0	<0.05	27.0	13.0	NA	0.0	41.6	58.4
PE/002391/2014	Pescara	6.3	0.23	33.0	7.8	<0.05	14.0	9.2	NA	0.0	86.0	14.0
PE/002392/2014	Pineto	4.6	0.18	41.0	10.0	<0.05	19.0	8.2	NA	0.0	42.6	57.4
PE/002393/2014	Pineto	6.3	0.17	45.0	12.0	<0.05	17.0	8.6	NA	0.0	71.9	28.1
PE/002481/2015	Giulianova	4.0	0.11	15.3	6.2	<0.05	9.1	6.8	NA	0.0	73.0	27.0
PE/002482/2015	Giulianova	4.6	0.13	13.9	4.8	<0.05	7.4	6.9	NA	0.0	84.2	15.8
PE/002483/2015	A. Adriatica	3.6	0.09	11.6	3.1	<0.05	5.3	6.1	NA	0.0	97.6	2.4
PE/002484/2015	A. Adriatica	5.9	0.11	13.5	3.7	<0.05	6.5	7.1	NA	0.0	91.2	8.8
PE/002485/2015	Pescara	5.2	0.12	12.2	3.5	<0.05	6.5	7.0	NA	0.0	89.8	10.2
PE/002488/2015	Pescara	5.1	0.13	12.6	3.4	<0.05	6.9	6.8	NA	0.0	92.5	7.5
PE/002490/2015	Pineto	3.6	0.08	15.3	4.3	<0.05	8.0	6.7	NA	0.0	87.5	12.5
PE/002492/2015	Pineto	4.6	0.12	26.6	8.6	<0.05	15.0	9.9	NA	0.0	64.2	35.8
PE/002540/2015	Ortona	4.9	0.10	11.6	3.5	<0.05	6.1	7.5	NA	0.0	93.4	6.6

PE/002541/2015	Ortona	5.2	0.23	48.1	16.5	0.05	26.1	12.5	NA	0.6	4.2	95.2
PE/002558/2015	Vasto	6.1	0.16	38.4	13.8	<0.05	21.3	11.0	NA	0.0	36.9	63.1
PE/002559/2015	Vasto	5.1	0.13	8.4	2.3	<0.05	4.5	5.7	NA	0.0	98.7	1.3
PE/002560/2015	San Salvo	5.3	0.11	7.9	2.7	<0.05	4.2	5.4	NA	0.0	99.1	0.9
PE/002561/2015	San Salvo	5.0	0.14	16.1	4.6	<0.05	8.0	7.0	NA	0.0	77.1	22.9
PE/006223/2016	Pescara	<2.0	0.46	23.9	3.4	<0.05	13.2	12.0	NA	NA	NA	NA
PE/006224/2016	Pescara	<2.0	0.25	15.8	2.9	<0.05	9.7	6.3	NA	NA	NA	NA
PE/006430/2016	A. Adriatica	2.2	0.45	40.9	17.0	<0.05	20.3	12.4	NA	NA	NA	NA
PE/006431/2016	A. Adriatica	<2.0	0.22	8.9	1.7	<0.05	6.2	5.5	NA	NA	NA	NA
PE/006432/2016	Giulianova	<2.0	0.21	22.7	6.4	<0.05	12.2	8.7	NA	NA	NA	NA
PE/006433/2016	Giulianova	<2.0	0.30	15.3	4.1	<0.05	7.7	8.9	NA	NA	NA	NA
PE/006514/2016	Pineto	3.0	0.23	23.7	5.1	<0.05	12.3	9.6	NA	NA	NA	NA
PE/006516/2016	Pineto	5.2	0.23	20.4	5.5	<0.05	10.8	10.3	NA	NA	NA	NA
PE/006599/2016	San Salvo	6.7	0.21	9.2	2.8	<0.05	8.4	6.6	NA	NA	NA	NA
PE/006600/2016	San Salvo	3.7	0.20	15.0	5.3	<0.05	6.7	8.5	NA	NA	NA	NA
PE/006601/2016	Vasto	4.3	0.22	8.6	2.5	<0.05	3.4	7.1	NA	NA	NA	NA
PE/006602/2016	Vasto	2.9	0.21	39.4	16.6	<0.05	18.8	10.4	NA	NA	NA	NA
PE/006603/2016	Ortona	4.3	0.16	8.5	3.3	<0.05	4.4	7.0	NA	NA	NA	NA
PE/006604/2016	Ortona	<2.0	0.24	46.4	14.3	<0.05	22.0	10.0	NA	NA	NA	NA
PE/002533/2012	Martinsicuro	16	0.15	80	20	0.09	49	16	72	NA	NA	NA
PE/002536/2012	A. Adriatica	24.0	0.12	44.0	11.0	<0.05	26.0	6.9	41.0	0	54.1	45.9
PE/002540/2012	Giulianova	8.2	<0.05	35.0	9.4	<0.05	20.0	6.3	30.0	0	58.6	41.4
PE/002541/2012	Giulianova	15.0	0.12	81.0	20.0	0.08	49.0	14.0	75.0	0	4.4	95.6
PE/002546/2012	Silvi Marina	13.0	0.09	19.0	3.4	0.05	15.0	2.6	24.0	0	96.1	3.9
PE/002547/2012	Silvi Marina	13.0	0.11	27.0	5.5	0.05	16.0	4.2	25.0	0	86.9	13.1
PE/003340/2012	Francavilla	8.1	0.08	16.0	78.4	<0.05	10.0	2.3	16.0	0	91.1	8.9
PE/003365/2012	Ortona	15.0	0.15	74.0	18.0	0.07	44.0	14.0	66.0	0.2	35.3	64.5
PE/003367/2012	Ortona	13.0	0.14	66.0	18.0	0.07	41.0	11.0	63.0	0	4.8	95.2
PE/003369/2012	Fossacesia	9.2	0.08	9.3	2.1	<0.05	8.1	2.2	12.0	0	99	1
PE/003371/2012	Fossacesia	8.2	<0.05	22.0	5.6	<0.05	13.0	4.8	21.0	0	87.2	12.8
PE/003375/2012	Fossacesia	14.0	0.17	87.0	23.0	0.09	52.0	18.0	82.0	0	11.7	88.3
PE/003441/2012	Vasto	9.0	0.17	88.0	22.0	0.15	50.0	17.0	83.0	0	1.5	98.5
PE/002535/2012	A. Adriatica	8.4	0.10	22.0	5.8	<0.05	13.0	4.2	20.0	0	85.7	14.3
PE/002551/2012	Pescara	12.0	0.10	28.0	6.4	<0.05	17.0	4.9	36.0	0	77.8	22.2
PE/003364/2012	Ortona	11.0	0.15	65.0	20.0	0.06	39.0	11.0	64.0	0	20.5	79.5
PE/003432/2012	Vasto	6.1	0.06	9.1	1.9	<0.05	6.4	1.8	9.4	0	99	1

769

770

771 **Table 2** Mineralogical composition, total organic content (TOC) and granulometry (wt%) of a subset of collected samples.

Label	Nearby town	Mineralogical Composition								TOC	Gravel	Sand	Mud	Outliers
		Quartz	Calcite	Dolomite	Plagioclase	Feldspars	Rutile	Muscovite	Chlorite-Smectite					
PE/005830/2016	Casalbordino	24.7	23.1	11.0	20.8	0.0	4.9	8.7	5.2	<0.5	0.0	49.5	50.5	
PE/005831/2016	Casalbordino	32.5	17.2	11.8	27.0	0.0	6.4	4.0	0.3	<0.5	0.0	85.7	14.3	
PE/005832/2016	Casalbordino	27.3	51.1	3.9	6.7	0.0	3.1	5.9	1.1	<0.5	0.0	51.9	48.3	
PE/005973/2016	Pineto	37.2	19.0	11.3	17.4	0.0	10.0	2.8	1.9	<0.5	0.0	89.1	10.9	
PE/005974/2016	Pineto	39.0	24.9	5.6	5.6	0.0	2.0	13.9	6.9	0.9	0.0	21.3	78.7	Pb, Cd
PE/005975/2016	Pineto	34.1	24.4	8.1	11.9	0.0	2.5	12.2	6.8	0.55	0.0	9.6	90.4	Pb, Cd
PE/000954/2016	Francavilla	47.0	19.9	11.2	15.4	0.0	4.0	2.0	0.0	0.78	0.0	97.2	2.8	
PE/000957/2016	Francavilla	44.1	11.4	4.7	26.3	0.0	9.8	3.0	0.1	0.69	0.0	95.3	4.7	
PE/000958/2016	Silvi Marina	24.2	11.8	13.3	37.8	0.0	8.0	0.6	3.9	0.66	0.0	95.9	4.1	
PE/000959/2016	Silvi Marina	32.0	14.0	9.7	34.0	0.0	6.0	3.1	0.7	1.13	0.0	96.3	3.7	
PE/006223/2016	Pescara	24.2	15.4	9.8	38.3	0.0	7.9	3.9	0.0					
PE/006224/2016	Pescara	31.9	21.2	14.0	18.5	0.0	3.1	5.5	5.1					
PE/006433/2016	Giulianova	27.7	19.1	4.0	34.7	0.0	7.0	6.8	0.2					
PE/006514/2016	Pineto	29.9	23.8	10.1	21.7	0.0	3.6	7.5	2.8					
PE/006516/2016	Pineto	26.9	24.2	6.0	24.4	10.0	5.1	1.9	1.0					
PE/006599/2016	San Salvo	27.3	30.7	8.6	20.9	0.0	8.8	3.4	0.0					
PE/006600/2016	San Salvo	32.2	23.3	9.7	20.6	0.0	5.5	6.0	0.9					
PE/006601/2016	Vasto	46.4	26.2	4.2	14.8	0.0	7.0	1.0	0.0					
PE/006602/2016	Vasto	24.2	25.7	11.5	21.0	0.0	8.4	6.9	1.1					
PE/006603/2016	Ortona	41.5	23.6	7.1	13.3	0.0	6.4	4.2	3.6					
PE/006604/2016	Ortona	35.7	23.2	8.4	16.9	0.0	3.0	5.9	5.0					
AVERAGE		32.9	22.5	8.8	21.3	0.5	5.8	5.2	2.2					
PRISMA campaign ^a	-	23	32.3	5.3	11	7	NA	13	2					

772 ^a Samples from PRISMA campaigns in the Abruzzo region as published by Spagnoli et al. (2014).

774 **Table 3**775 Reference threshold values (L_1 and L_2). according to the Italian Decree 173/2016 and local background776 calculated after this study (L_{1loc} and L^*_{1loc}). Values are expressed as $\mu\text{g g}^{-1}$ of dry matter.

777

778

779

Limit concentrations ($\mu\text{g/g d.m.}$)

Metal	L_1	L_{1loc}	L^*_{1loc}	L_2
As ^a	12.0	12.8	12.0	20.0
Cd ^a	0.3	0.4	0.3	0.8
Cr	50.0	65.0	65.0	150.0
Hg ^a	0.3	0.1	0.1	0.8
Ni	30.0	40.8	40.8	75.0
Pb	30.0	16.5	16.1	70.0
Cu	40.0	19.8	18.0	52.0
V	NA	77.4	77.4	NA
Zn	100.0	72.3	72.3	150.0

* after removing the outliers from distribution

^a computed with ROS method for censored data

780

781

782

783

784

785

786